NASA-CR-202561

OBSERVATIONS OF THE ROTATIONAL TRANSITIONS OF OH FROM THE ORION MOLECULAR CLOUD

IN-89-CR

004 995

Grant NAG2-311

Semiannual Report Nos. 11-20 and Annual Report Nos. 1-2

For the period 1 October 1989 through 30 September 1996

Principal Investigator:

Dr. Gary J. Melnick

September 1996

Prepared for the
National Aeronautics and Space Administration
Ames Research Center
Moffett Field, CA 94035-1000

Smithsonian Institution
Astrophysical Observatory
Cambridge, Massachusetts 02138-1596

The Smithsonian Astrophysical Observatory
is a member of the
Harvard-Smithsonian Center for Astrophysics

The NASA Technical Officer for this grant is Mr. Curtis D. Laughlin, Airborne Astronomy Branch, Code 211-12, NASA Ames Research Center.

Observations of the Rotational Transitions of OH from the Orion Molecular Cloud

Grant NAG2–311

Semiannual Report Nos. 11-20 and Annual Report Nos. 1-2

I. Introduction

The chemical makeup of the interstellar medium depends on the initial composition of the gas as well as the temperature and density history of the medium. For example, unperturbed cold gas – as might be found inside quiescent molecular clouds – is expected to chemically evolve in ways quite different from gas exposed to the higher temperatures and densities of cloud cores undergoing star formation. The most common and violent perturbation to the chemical evolution of the interstellar medium is the passage of a shock wave, which can rapidly compress and heat the gas in its path. However, a critical difference exists between shocks of different velocities; whereas slower shocks lack the energy to destroy pre-existing molecules and dust grains, faster shocks have sufficient energy to dissociate all molecules and grain mantles they encounter. Thus, shocks of different strengths are predicted to leave measurably different chemical compositions in their wakes. In this way, a study of the emission spectrum (and therefore the composition) of star-forming regions can be used to infer the dynamics of the gas when either the scale of the moving gas is too small to be spatially resolved or the geometry of the region is too complex to be easily untangled.

Few other molecules serve this diagnostic purpose better than OH and SiO. First, because dissociative shocks ($v_{\rm shock} \geq 50$ km s^{-1}) return large amounts of Si and O previously tied up in other molecules and silicate grains to the medium, SiO is predicted to be produced in relatively high abundance only behind such shocks. (During the subsequent re-formation of molecules in the warm post-shocked gas, chemical reactions leading to the formation of SiO proceed much more rapidly than in the cold interstellar medium.) Similarly, the OH abundance is predicted to be enhanced behind dissociative shocks. Second, because SiO lines are not emitted from H II regions or photodissociation regions (unlike [OI], [Si II], and the hydrogen recombination lines), the detection of SiO implies emission from shocked gas, simplifying the interpretation of observations of high-J SiO in star-forming clouds. Finally, OH has several transitions at far-infrared wavelengths while SiO has a large number of observable transitions at millimeter, submillimeter, and far-infrared wavelengths that span a range of temperatures above the ground state that are of great diagnostic value (see Fig. 1). The study of OH covered by this grant is complete and has been documented in a number of published papers:

"Observations of Rotational Transitions of OH from OMC-1", Gary Melnick, in *Masers, Molecules, and Mass Outflows in Star Forming Regions*, ed. A.D. Haschick

(Haystack Observatory Press), p. 33 (1986).

"Observations of Far-Infrared Line Profiles in the Orion-KL Region", Michael K. Crawford, John B. Lugten, W. Fitelson, Reinhard Genzel, and Gary Melnick, *Ap. J.*, **303**, L57 (1986).

"The Rotational Excitation of OH in Orion", Ewine F. van Dishoeck, Gary J. Melnick, and John H. Black, in *Star Forming Regions*, Proceedings of IAU Symposium No. 115, eds. M. Peimbert and J. Jugaku (Reidel), p. 176 (1987).

"Interpretation of Rotationally Excited, Far Infrared OH Emission in Orion-KL", Gary J. Melnick, Reinhard Genzel, and John B. Lugten. *Ap. J.*, **321**, 530 (1987).

"Far-Infrared, Rotationally Excited OH Emission in Orion-KL", Gary J. Melnick, Reinhard Genzel, Albrecht Poglitsch, Gordon J. Stacey, and John B. Lugten, in *Interstellar Matter*, Proceedings of the Second Haystack Observatory Conference, eds. J. M. Moran and P. T. P. Ho (Gordon and Breach), p. 187 (1988).

"Infrared Line Emission from High-Velocity Outflows in Star Forming Regions", Gary J. Melnick, in *Infrared Spectroscopy in Astronomy*, ed. M. F. Kessler (ESA Publications SP-290), p. 259 (1989).

"Further Observations of Rotationally Excited, Far-Infrared ^{16}OH and ^{18}OH Emission in Orion-KL: Tighter Constraints on the Nature of the Emitting Region", Gary J. Melnick, Gordon J. Stacey, Reinhard Genzel, Albrecht Poglitsch, and John B. Lugten, *Ap. J.*, **348**, 161 (1990).

The purpose of the remaining work covered in this grant has been to observe, and when possible map, the emission from several high$-J$ transitions of SiO towards Orion-KL in order to determine the extent and magnitude of the effects of high velocity shocks in the core of Orion.

II. Status of SiO Work

As indicated above, to extract the most science from the KAO observations of the $J = 25 - 24$ SiO line it was useful to observe several other SiO lines of intermediate $J-$value. This is helpful for two reasons. First, a much more accurate model of the emitting region can be constructed when such a model must reproduce more than one line strength. Second, though at a much higher frequency than any ground-based SiO observation, the spatial resolution of the KAO at 1083 GHz, the frequency of the $J = 25 - 24$ SiO observations, is 76.5 arcseconds (set by the diffraction limit of the 0.91-cm diameter KAO primary mirror) and is less than that obtainable from either the 10.4-m diameter Caltech Submillimeter Observatory (CSO) or the 15-m diameter James Clerk Maxwell Telescope (JCMT) operating at lower frequencies. Therefore, the supplemental mountain-top observations have also been used to obtain higher spatial resolution maps of the SiO emission than was possible with the KAO.

Because of limited observing time at the CSO and JCMT and the unavailability of sensitive receivers at frequencies greater than 600 GHz until recently, obtaining these additional measurements has taken longer than first anticipated. However, these measurements are now complete. A summary of these observations is given in Table 1 and the KAO spectrum along with some of the mountain-top results are shown in Figures 2–4.

TABLE 1. Summary of High−J SiO Observations

J_u − J_ℓ	Frequency (GHz)	Telescope	Spatial Resolution (arcseconds)
25 − 24	1083.7344	KAO	76.5
16 − 15	694.2945	CSO [1]	10.4
16 − 15	694.2945	JCMT [2]	7.2
15 − 14	650.9566	CSO	11.1
14 − 13	607.6080	CSO	11.9
8 − 7	347.3306	CSO	20.9

[1] Caltech Submillimeter Observatory
[2] James Clerk Maxwell Telescope

In addition to these observations, the computer code needed to model emission behind fast (J−type) shocks has been completed and tested. The only remaining work is to write the final paper, which has begun. We estimate that the SiO work could be concluded in about two months. However, Dr. Melnick's responsibilities as the Principal Investigator on the Submillimeter Wave Astronomy Satellite (SWAS) prohibit him from spending all of his time on the SiO effort and with the launch of SWAS scheduled for the early part of 1997 and activities leading to launch increasing, it is unlikely that this situation will substantially change in the near future. Nonetheless, we do expect to be able to spend enough time on the task to complete it within this next year.

III. Figures

FIGURE 1. Plot of the frequency distribution of SiO transitions (*bottom panel*), and the energy above the ground state for each transition (*top panel*).

FIGURE 2. SiO $J = 25 - 24$ spectrum towards Orion-KL obtained from the KAO.

FIGURE 3. SiO $J = 8 - 7$ spectra towards Orion H_2 Peak 1 (*top*), IRc2 (*middle*), and H_2 Peak 2 (*bottom*).

FIGURE 4. Map of the integrated main beam brightness temperature of the SiO $J = 8 - 7$ line between -24 and $+42$ km s^{-1} (*top panel*). The (0,0) position of the map is centered on IRc2, R.A. = 5:32:46.8 and DEC = -5:24:25.0 (1950.0); right ascension cut along dotted axis (*middle panel*); declination cut along dotted axis (*bottom panel*).

FIGURE 5. Velocity channel maps of SiO $J = 8 - 7$ emission: -24 to -2 km s^{-1} (*left panel*); -2 to $+20$ km s^{-1} (*center panel*); $+20$ to $+42$ km s^{-1} (*right panel*).

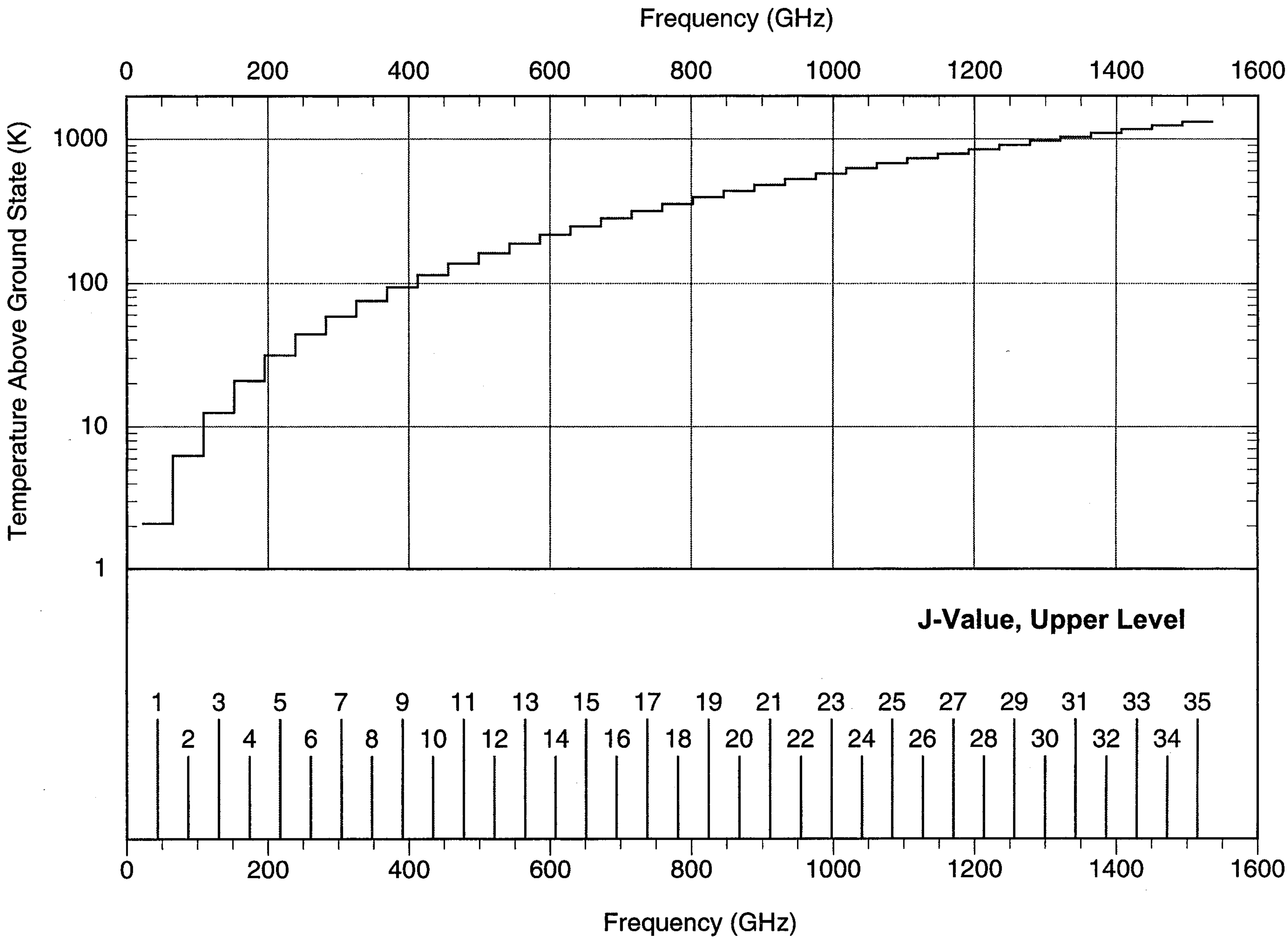
Frequency (GHz)
0
200
400
600
800
1000
1200
1400
1600
Temperature Above Ground State (K)
1000
100
10
1
J-Value, Upper Level
1 3 5 7 9 11 13 15 17 19 21 23 25 27 29 31 33 35
2 4 6 8 10 12 14 16 18 20 22 24 26 28 30 32 34
0
200
400
600
800
1000
1200
1400
1600
Frequency (GHz)

Fig. 1

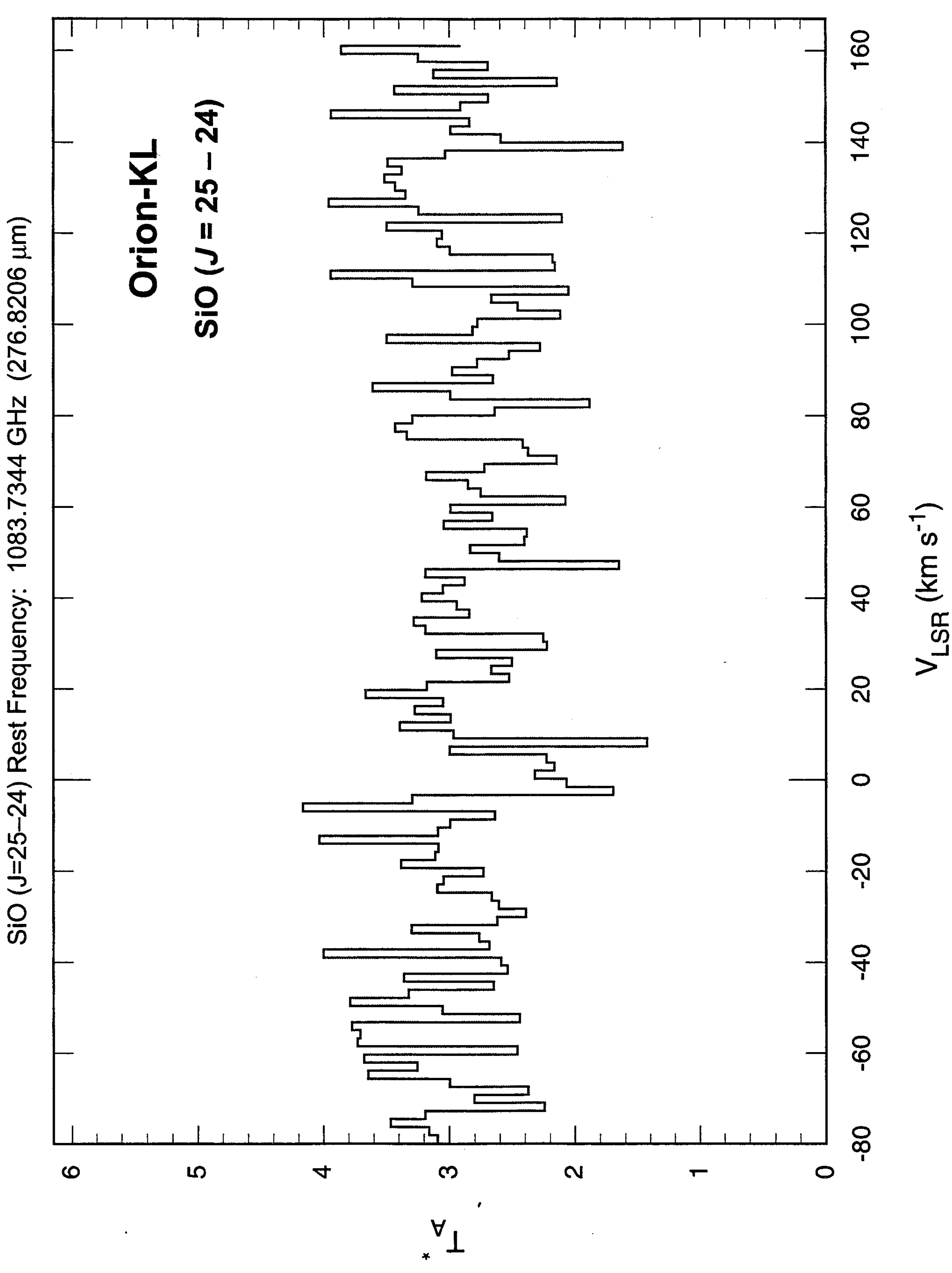
SiO (J=25–24) Rest Frequency: 1083.7344 GHz (276.8206 μm)
Orion-KL
SiO (J = 25 – 24)
T_A^*
V_{LSR} (km s^{-1})
0
1
2
3
4
5
6
-80
-60
-40
-20
0
20
40
60
80
100
120
140
160

Fig. 2

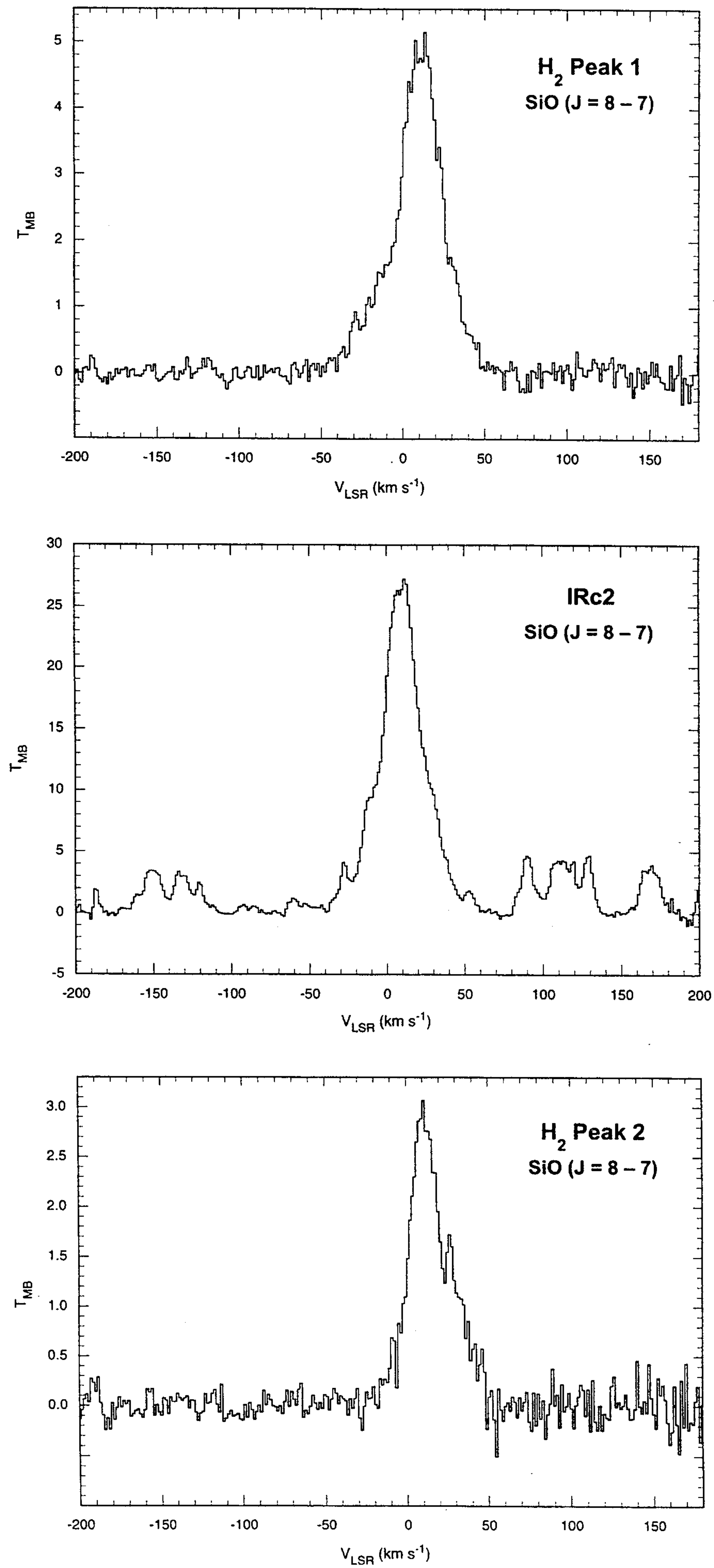
H2 Peak 1
SiO (J = 8 – 7)
T_MB
V_LSR (km s^-1)
IRc2
SiO (J = 8 – 7)
T_MB
V_LSR (km s^-1)
H2 Peak 2
SiO (J = 8 – 7)
T_MB
V_LSR (km s^-1)

Fig. 3

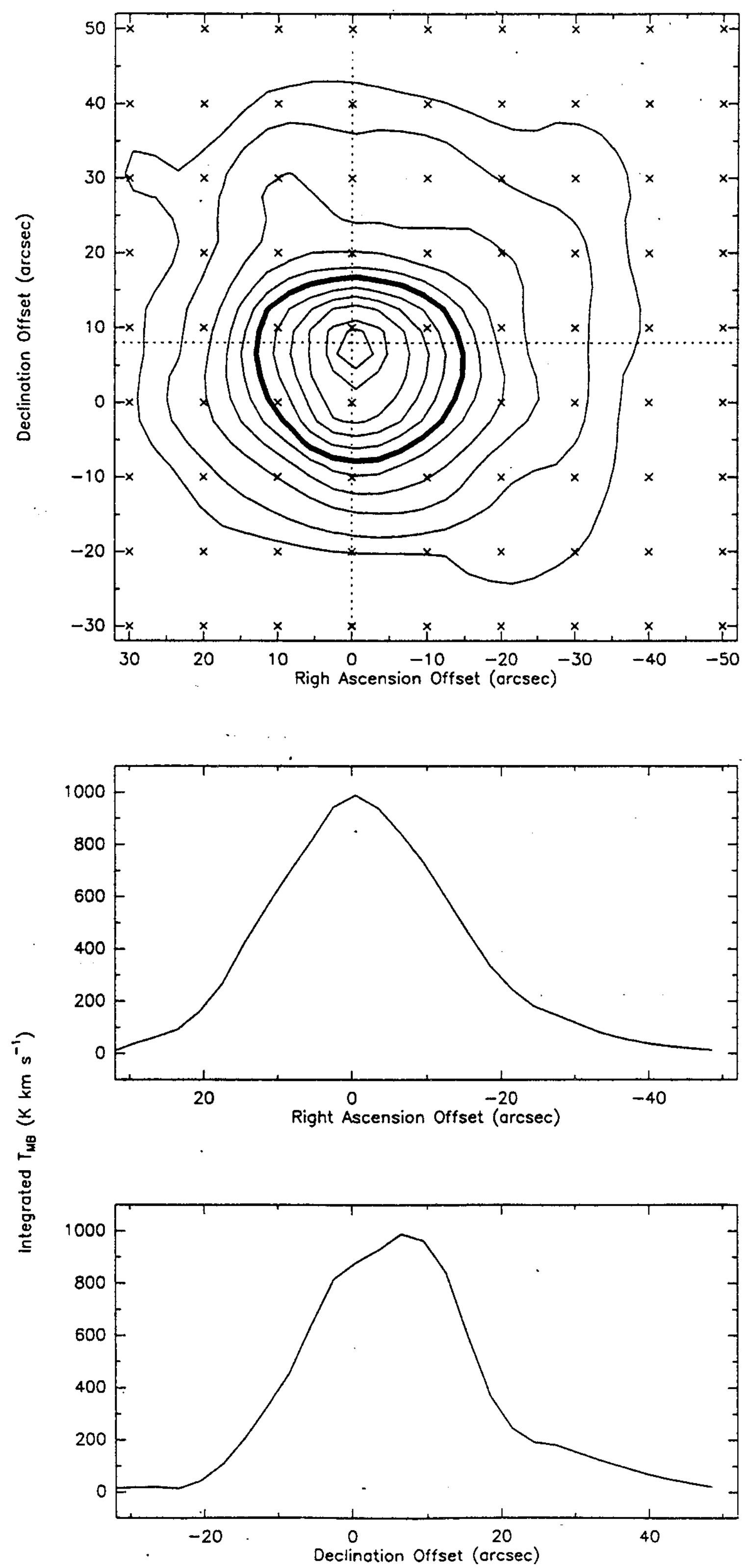
Declination Offset (arcsec)
Righ Ascension Offset (arcsec)
Integrated T_{MB} (K km s^{-1})
Right Ascension Offset (arcsec)
Declination Offset (arcsec)

Fig. 4

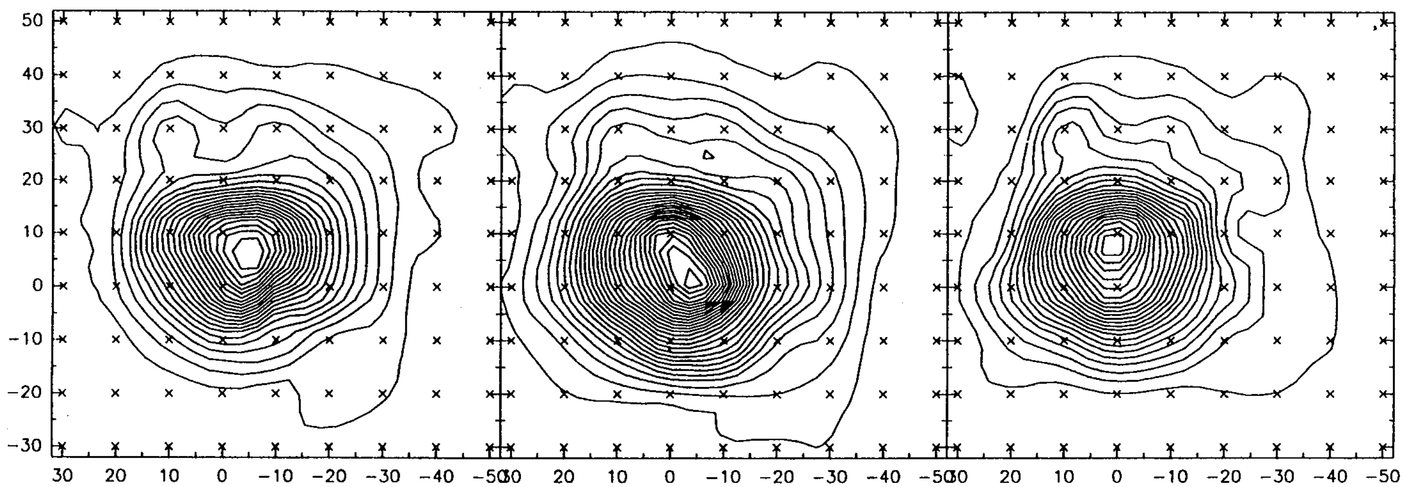

Fig. 5